ELSEVIER

Nuclear Medicine and Biology 30 (2003) 177–186

NUCLEAR MEDICINE — AND — BIOLOGY

www.elsevier.com/locate/nucmedbio

Quantification of brain μ-opioid receptors with [^{11}C]carfentanil: reference-tissue methods

Christopher J. Endres, Badreddine Bencherif, John Hilton, Igal Madar, J. James Frost*

Department of Radiology, Johns Hopkins University, Baltimore, MD 21287, USA

Received 16 August 2002; received in revised form 19 September 2002; accepted 19 September 2002

Abstract

[^{11}C]Carfentanil (CFN) is a μ-opioid agonist used for *in vivo* positron emission tomography (PET) studies of μ-opioid receptors. Previously, a tissue-ratio method was validated for the quantification of CFN binding. However, since that initial validation, several other blood independent (reference-tissue) methods have become available. To evaluate these methods, CFN PET studies with arterial blood sampling were acquired in six healthy male control subjects. Specific binding estimates obtained from reference-tissue methods were compared to those obtained with a more rigorous blood input modeling technique. It was determined that both a graphical method, and a simplified reference tissue model, were more accurate than the tissue-ratio method for quantification of CFN binding.

Keywords: Mu-opioid receptors; Opiates; [^{11}C]carfentanil; Positron emission tomography

1. Introduction

[^{11}C]Carfentanil (CFN) is a reversible μ-opioid agonist and is one of the first receptor binding ligands to be studied with positron emission tomography (PET) [6]. An early evaluation of CFN kinetics showed that a simple tissue-ratio method provides estimates of CFN binding that are highly correlated ($r = 0.98$) with specific binding estimates obtained using a more rigorous blood-input modeling technique [7]. The tissue-ratio method uses the tracer activity concentration in occipital cortex, a region that contains a negligible concentration of μ-opioid receptors [9], to correct for non-specific binding. Because invasive blood sampling is not required for analysis, the tissue-ratio method was seen as an attractive approach. However, since the original validation of the tissue-ratio method several blood independent 'reference-tissue' techniques have been developed to measure receptor binding for reversible ligands, including reference-tissue modeling [15,16,22], graphical analysis [18], and multilinear fitting [11]. Unlike the tissue-ratio method, these more recently developed reference-tissue techniques can all be derived from blood-input compartmental modeling. Although the newer reference-tissue methods only approximate the more rigorous blood-input methods, they still are expected to be more accurate than using simple tissue-ratios which have been shown to systematically produce a biased measurement of total tissue binding [2]. However, quantitative methods always need to be carefully evaluated for each individual tracer, and since the tissue-ratio method has already been validated for CFN it is not certain that another method will provide a significantly more accurate or reliable measurement. To make a more conclusive determination, we have applied several reference-tissue and blood-based quantitative methods to measure CFN specific binding in six healthy human subjects. CFN uptake in mouse brain was also examined to resolve an outstanding issue regarding the possible cerebral uptake of radioactive metabolites.

2. Materials and methods

2.1. Human subjects

Six healthy male volunteers (ages 20-29 years) were included in this study. The Johns Hopkins Joint Committee on Clinical Investigation approved the protocol, and all subjects provided signed consent prior to entry in the study.

* Corresponding author. Tel.: +(410) 955-8449; fax: +(410) 614-3896.

E-mail address: jfrost@jhmi.edu (J.J. Frost).

0969-8051/03/$ – see front matter
PII: S0969-8051(02)00411-0

2.2. Image acquisition

A thermoplastic mask was individually fitted to each subject's face for the purpose of immobilization and positioning during the scans. Prior to the day of PET scanning, MR images were acquired using a 1.5 T Signa Advantage system (GE Medical Systems, Milwaukee, WI, U.S.A.) and a three-dimensional SPGR (Spoiled Gradient Recalled Acquisition in the Steady State) sequence with the following parameters; repetition time 50 ms; echo time 5 ms, flip angle of 45 degrees, number of excitations 1; field of view of 24 x 24 cm; slice thickness = 1.5 mm; reconstruction matrix of 256 x 256, yielding an in-plane pixel size of 0.93x0.93 mm. MRI scans were applied for PET structural localization using a standard technique [19]. For the PET studies, the subjects were positioned in the scanner using a landmark previously determined by MRI. A 10-min transmission scan was obtained prior to tracer injection. [^{11}C]Carfentanil (CFN) was synthesized via the reaction of [^{11}C]methyliodide and a nor-methyl precursor as previously described [3]. An intravenous bolus administration of 19.0 ± 1.5 mCi (17-22 mCi) CFN with a specific activity of 4807 ± 1303 mCi/μmole (3082-6941 mCi/μmole) was administered through a 0.9% sodium chloride IV catheter. PET data were acquired on a GE Advance scanner (General Electric, U.S.A.) in 3D mode, which acquires 35 simultaneous slices with an interslice separation of 4.25 mm [4]. Twenty-five sets of scans were acquired over ninety minutes (6x30 sec, 5x60 sec, 5x120sec, 9x480sec). The positioning of the patient was continuously monitored and, if necessary, was corrected by repositioning. PET image data were reconstructed using a ramp reconstruction filter and a 25.6 cm by 25.6 cm field of view into 128 x 128 pixel matrix. The final resolution at full width half maximum (FWHM) with these parameters is 5 mm in-plane. Images were decay corrected to the time of injection.

2.3. Blood sampling

Following bolus injection of CFN, blood was sampled from a radial arterial catheter as fast as possible for the first 2 min, then at times of 3, 4, 5, 6, 7, 8, 10, 12, 14, 16, 20, 25, 30, 35, 40, 50, 60, 75, and 90 min post-injection. The blood sampling volume was 1.5 ml, with larger samples (8 ml) taken at 5, 10, 20, 30, 40, 60, and 90 min to provide additional blood for radioactive metabolite analysis. To measure plasma radioactivity, whole blood samples were centrifuged and 0.5 ml plasma was counted for 1 min in a NaI well counter (CompuGamma CS by Wallac Oy, Turku, Finland). For the assay of radioactive metabolites, plasma from heparinized blood was analyzed by a column–switch HPLC method [10]. For this procedure 4 ml plasma was first passed through a small capture column packed with Oasis sorbent (Waters Corp. Milford, MA). The capture column was washed with 1% acetonitrile in water before the solutes, which were retained by the column, were swept onto an analytical column (Sphereclone C8, 150x4.6 mm, Phenomenex, Torrance, CA) by 75% acetonitrile in 50mM sodium phosphate buffer pH 5.5 at a flow rate of 1.4 ml/min. Radioactivity was detected in the column effluents by a dual BGO detector with a 0.25 ml flow cell (Bioscan, Washington DC).

2.4. Data analysis

PET images were processed with Analyze™ software (Mayo foundation, Rochester, MN) on SUN Ultra 10 workstations. The placement of regions-of-interest (ROIs) was based on subject PET scan anatomy and SPGR MRI images. The MRI images were coregistered to a mean PET image (average of all scans) using the registration software in SPM 99. Square 4x4 pixel ROIs were placed on the cortical and subcortical regions using the coregistered MRI images. For occipital cortex, 8x8 pixel ROIs were used. The ROIs were then applied to the PET images to generate time activity curves. ROIs were placed on the following structures: amygdala (AMY), caudate (CAU), cerebellum (CER), cingulate cortex (CIN), frontal cortex (FRO), occipital cortex (OCC), parietal cortex (PAR), putamen (PUT), temporal cortex (TEM), peri-aqueductal gray matter (PAG), and thalamus (THA). Both tissue and blood activity were decay corrected to the time of injection. Measured plasma metabolite fractions were fit to the function $M_F(t)=a_1 t/(a_2+t)$, where a_1 and a_2 are fitted parameters. To obtain an input function, $M_F(t)$ was used to correct all plasma samples for radioactive metabolites. For one subject there was an error in metabolite processing, thus the average metabolite fractions measured in the other 5 subjects was used to perform metabolite correction, which was justified by the small deviations of the metabolite fractions measured across subjects (see Results).

2.5. Compartmental analysis

Compartmental modeling with a blood input function was applied to characterize the tissue kinetics of CFN, and to obtain BP estimates to be used for comparison with reference-tissue based estimates. The initial step in compartmental modeling was to estimate the non-specific volume of distribution (V_e) from OCC, a region that is devoid of μ-opioid receptors. OCC was fit to both a one-tissue model (K_1^r, k_2^r, V_b) and a two-tissue model (K_1^r, k_2^r, k_5, $ns=k_5/k_6$, V_b) (Figure 1), with a fitted blood volume term (V_b) included to account for vascular radioactivity. For example, for the one-tissue model OCC was fit to the equation $K_1^r C_p \otimes \exp(-k_2^r t)+V_b C_{wb}$, which was integrated over each PET frame interval. K_1^r and k_2^r are first order rate constants describing the bidirectional flux of tracer between blood and tissue, C_{wb} is the whole blood radioactivity concentration, C_p is the metabolite corrected plasma activity, and $\otimes$ denotes mathematical convolution. The two-tissue model also includes first order rate constants (k_5, k_6) that

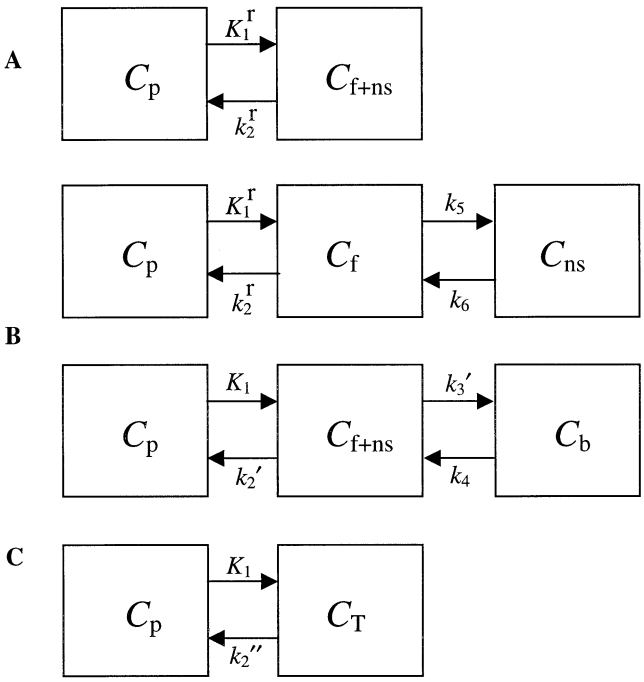

Fig. 1. Compartmental models used to quantify [^{11}C]carfentanil (CFN) binding potential. **A:** One-tissue model for a region with no specific binding. The model features a plasma compartment (C_p) and a single tissue compartment (C_{f+ns}) that represents free+non-specifically bound tracer. The first order rate constants K_1^r and k_2^r describe bidirectional tracer flux between blood and tissue. In the present work model A was exclusively applied to time-activity curves in occipital cortex (OCC), a region that is nearly devoid of μ-opioid receptors, in order to estimate the non-specific volume of distribution (V_e) which is K_1^r/k_2^r. **B:** Two-tissue model for a region with no specific binding. Model B includes separate tissue compartments for free (C_f) and non-specifically bound (C_b) tracer, with rate constants k_5 and k_6 describing bidirectional flux between C_f and C_b. As with model A, model B was applied to OCC in order to estimate V_e, which for model B is equal to $K_1^r/k_2^r(1+k_5/k_6)$. **C:** Two-tissue model for a specific binding region. Model C includes tissue compartments for free+non-specifically bound (C_{f+ns}), and specifically bound (C_b) ligand. Using the notation of Koeppe et al. (1991), first order rate constants describe blood-tissue exchange (K_1, k_2'), receptor binding (k_3'), and dissociation (k_4). The non-specific volume of distribution (V_e) is equal to K_1/k_2', and the binding potential is k_3'/k_4. Model C was used to fit time-activity curves in specific binding regions, with V_e fixed to a value previously measured in OCC using models A or B. **D:** One-tissue model for a specific binding region. Model D is a simplification of model C, where it is assumed that receptor binding and dissociation are sufficiently rapid such that compartments C_{f+ns} and C_b are in transient equilibrium. As a result, they are kinetically indistinguishable and can thus be lumped into a single tissue compartment $C_T = C_{f+ns}+C_b$. The parameter k_2'' is a net efflux rate that is related to the rate constants of model C by $k_2'' = k_2'/(1+k_3'/k_4)$. Model D has the advantage of reducing the number of fitted parameters, and is commonly used to represent the tissue activity of specific binding regions for application of reference-tissue modeling approaches. For example, a common reference-tissue method is derived using model A for the reference-tissue and model D for the specific binding region (Lammertsma et al., 1996). The model parameters for this method are $R_1=K_1/K_1^r$, k_2', and $BP=k_3'/k_4$. An alternative approach uses two-tissue compartments (model B) for the reference region with parameters R_1, k_2', k_5, k_6 and BP (Watabe et al., 2000).

describe tracer flux for a distinct non-specific binding compartment (Figure 1B). Fitting weights (W_i) were computed from $W_i=\exp(-\lambda t)\Delta t_i/C_i(t)$, where λ is the radioactive decay constant of ^{11}C (20.38 min), Δt_i is the time interval of the ith scan frame, and C_i is the tissue-activity measured in a large brain ROI that includes both gray and white matter. Time-activity curves were fit for the entire study duration (0-90 min). The one-tissue and two-tissue model V_e estimates are computed from K_1^r/k_2^r and $K_1^r/k_2^r(1+k_5/k_6)$, respectively. The value of V_e was derived from the model that gave the best fit to OCC as judged by the Akaike information criterion [1]. Subsequent to modeling of OCC, other time-activity curves were fit to a two-tissue model (Figure 1C), with K_1/k_2' fixed equal to V_e. This produced estimates of K_1, k_3', k_4, BP_{CM} (k_3'/k_4), and V_b in specific binding regions. We report regional parameter values (mean±sd), and their average standard fitting errors.

2.6. Estimation of BP

Six methods were applied for estimating the binding potential (BP) of CFN: (I) Compartmental modeling with a blood input function as described above ($BP_{CM} = k_3'/k_4$). (II) Logan graphical analysis with a blood input function [17]. From the linear slopes obtained from OCC (S_{OCC}) and a specific binding region (S_{SB}), the BP estimate is $BP_L = (S_{SB}-S_{OCC})/S_{OCC}$. (III) Logan graphical analysis with a reference-tissue input function (OCC), for which BP is computed from $BP_{LR} = DVR - 1$. DVR, which is equal to the fitted linear slope, is the ratio of the total distribution volumes in target and reference tissues [18]. For this method, BP_{LR} was computed with both $k_2'=0$, and k_2' set to the average value (0.104 min^{-1}) obtained from the modeling procedure performed in method I. To examine the effect of a delayed approach to linearity of the Logan plot, slopes measured with methods II and III were obtained using 10-90, 20-90, and 30-90 min of data. (IV) A simplified reference-tissue model that is derived from one-tissue models for both the reference (Figure 1A) and specific binding (Figure 1D) regions [16]. With this method specific-binding regions were fit using OCC as a reference-tissue input function to estimate R_1, k_2', and BP_{SRTM}. Fits were weighted as described in method I. To reduce the effects of vascular activity, tissue curves were fit from 1-90 min. A four-parameter reference-tissue model was also tested [15], however, the results were nearly identical to those obtained with the simplified method and are not reported separately. (V) A modification of the simplified reference-tissue model, for which the reference-tissue is modeled using 2 tissue compartments (Figure 1B) [22]. Referring to the parameter notation in Figures 1B and 1D, the operational equation for this method is given by $C_t = R_1[C^r_t + aC^r_t \otimes \exp - (k_5 + k_6)t + bC^r_t \otimes \exp - k_2''t]$, where $R_1=K_1/K^r_1$, $C^r_t=C_f+C_{ns}$ is the total reference tissue concentration, $a=k_5k^r_2/(k_5 + k_6 - k_2'')$, $b=(k_2''k_2'' - k_2''(k^r_2 + k_5 + k_6) + k_6) + k_6k^r_2)/(k_5 + k_6 - k_2'')$, and $BP_{R2TM}=R_1k^r_2/(k_2''(1 + k_5/k_6))-1$. In our

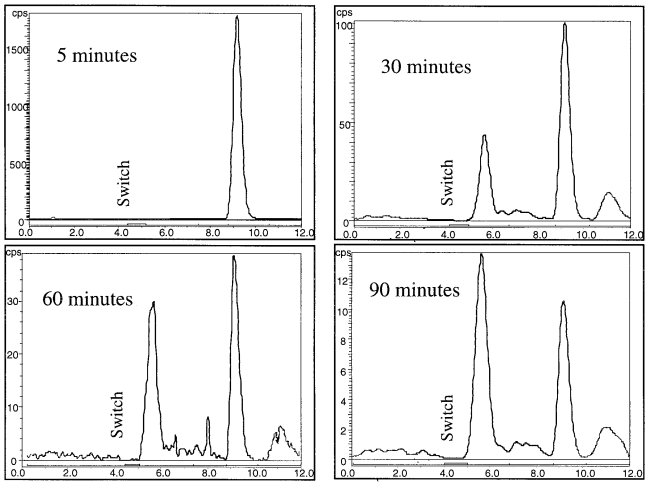

Fig. 2. HPLC chromatograms of plasma radioactive metabolites at 5, 30, 60, and 90 min following bolus injection of [^{11}C]carfentanil. For metabolite analysis, a column switching technique was used (see text) in which plasma samples are first loaded onto a capture column, and are then flushed through an analytical column. [^{11}C]Carfentanil elutes at about 5 min following the column switch. The primary metabolite elutes at 1.5 min following the switch indicating it is more polar than [^{11}C]carfentanil. A minor metabolite eluted at 7 min which indicates that it is more lipophilic than [^{11}C]carfentanil, and thus is a potential candidate for crossing the blood-brain barrier.

implementation, the regression equations were expressed in terms of the five parameters R_1, k_2^r, k_5, ns=k_5/k_6, and BP_{R2TM}. The fitting process for this method is a two-step procedure. In step 1, the cortical regions as well as cerebellum are fit (with OCC input) to estimate R_1, k_2^r, ns, and BP_{R2TM}, with k_5 fixed to a value of 0.05 min^{-1}. In step 2, the mean fitted values of k_2^r and ns, obtained in step 1, as well as k_5, are held fixed, then R_1 and BP_{R2TM} are estimated for all tissue regions. (VI) Tissue-ratio method [7]. With this method BP is calculated from $BP_{RATIO} = (TAC_{SB}-TAC_{OCC})/TAC_{OCC}$, where TAC_{SB} and TAC_{OCC} are the time-activity curves (average of 34-82 min) in a specific binding region and OCC, respectively.

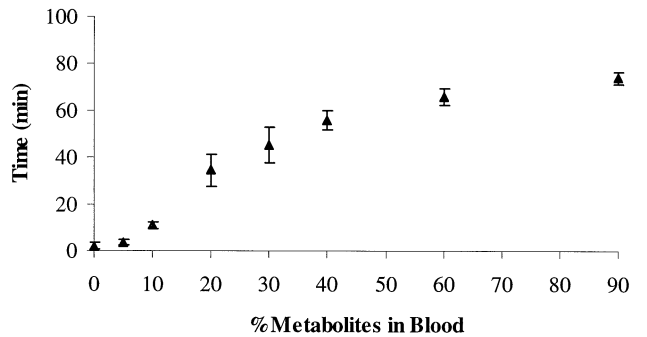

Fig. 3. Percent radioactive metabolites in blood (n = 5) following bolus injection of [^{11}C]carfentanil (mean±sd). By 40 min post-injection, radioactive metabolites account for more than 50% of the total plasma radioactivity.

2.7. Simulations

Simulated CFN time-activity curves were used to investigate the effects of blood flow on estimation of BP. Using a two-tissue model (Figure 1C), noise-free time-activity curves were simulated using mean values of V_e, k_4, and V_b obtained from compartmental modeling. Several values of k_3' were selected based on the range of fitted values obtained throughout the brain. To simulate a change in blood flow, K_1 and k_2' were varied simultaneously, with the value of V_e (K_1/k_2') held fixed to the mean fitted value. K_1 was varied over a wide range that extended beyond the range of fitted values. Simulated curves were analyzed with methods II-VI, and the ratios of the estimated and true BP values were plotted vs. K_1.

2.8. Mouse studies

Three male CD1 mice (Charles River) weighing 23-25g were given 500μCi CFN (specific activity 5000-8000 Ci/mmole) intraperitoneally. Twenty minutes later the mice were killed by cervical dislocation and were then exsanguinated into a weighing boat containing 100uL heparin solution (100U/ml). Plasma was prepared by centrifugation. The brain was quickly removed, rinsed in cold saline, and homogenized into 0.8 ml acetonitrile. The homogenate was centrifuged for 2 min in a microcentrifuge(13,000xg). The plasma and brain extract were analyzed by column switch HPLC as described in Section 2.3. For plasma analysis, 0.2-0.3 ml plasma, diluted to 4 ml with water, was introduced into the column switch HPLC. Similarly 0.2-0.4 ml of the brain extract was analyzed.

3. Results

3.1. Blood metabolite data

Figure 2 shows HPLC chromatograms of CFN and its radioactive metabolites. Plasma contained one major me-

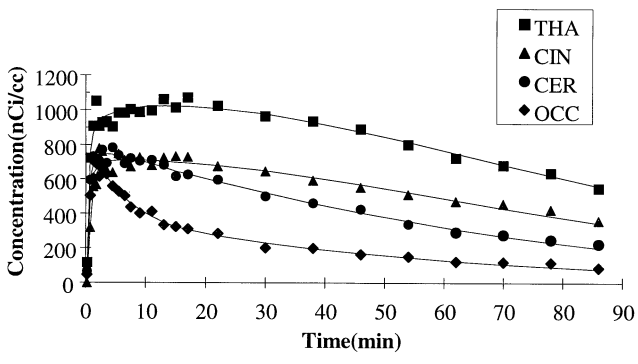

Fig. 4. Fitted [^{11}C]carfentanil tissue time-activity curves using the two-tissue model shown in Figure 1. The displayed regions are thalamus (THA [■), cingulate (CIN ▲), cerebellum (CER ●), and occipital cortex (OCC ◆). The non-specific volume of distribution (V_e) was estimated from the model fit in OCC. For fitting all other regions, K_1/k_2' was fixed to V_e. All fitted curves included a blood volume term.

Table 1
Fitted parameter values for [^{11}C]carfentanil (n=6) obtained using a two-tissue compartmental model (Figure 1C). The table shows mean values with standard deviations in parentheses.

	K_1 (mL/min/mL)	k_3' (min^{-1})	k_4 (min^{-1})	V_b (mL/mL)
Amygdala	0.129 (.017)	0.334 (.323)	0.084 (.072)	0.037 (.015)
Caudate	0.183 (.029)	0.348 (.140)	0.091 (.017)	0.037 (0.12)
Cerebellum	0.168 (.014)	0.177 (.039)	0.134 (.036)	0.042 (.008)
Cingulate	0.157 (.025)	0.246 (.139)	0.151 (.097)	0.049 (.025)
Frontal cortex	0.161 (.018)	0.143 (.087)	0.107 (.030)	0.040 (.010)
Peri-acqueductal grey	0.141 (.018)	0.225 (.225)	0.127 (.123)	0.041 (.017)
Parietal cortex	0.157 (.022)	0.120 (.068)	0.108 (.036)	0.045 (.007)
Putamen	0.200 (.029)	0.312 (.166)	0.120 (.041)	0.037 (.027)
Temporal cortex	0.146 (.018)	0.182 (.145)	0.133 (.053)	0.040 (.008)
Thalamus	0.214 (.036)	0.335 (.109)	0.090 (.039)	0.035 (.018)

tabolite, which eluted 1.6 min following the column switch and accounted for 37% of the total plasma radioactivity at 60 min following injection of CFN. A minor metabolite (13% of total at 60 min) eluted at 7 min and was more lipophilic than CFN itself, which eluted 5.2 min following column switch. The lipophilic metabolite was grouped with other (less lipophilic) metabolites and is included in the average total metabolite fractions shown in Figure 3. By 40 min post-injection radiolabelled metabolites account for more than 50% of the plasma radioactivity.

3.2. Compartmental modeling

The two-tissue model yielded good fits for all tissue regions (Figure 4). In all subjects the occipital cortex was better fit to a two-tissue model than a one-tissue model, as judged by the Akaike information criterion. Thus the total OCC distribution volume measured with the two-tissue model served as an estimate of the non-specific distribution volume (V_e). The average value of V_e across subjects (mean $\pm$ sd) was 1.59 $\pm$ 0.27 mL/mL, with a standard fitting error of 0.12 ml/mL. The fitted parameter values measured in specific binding regions are shown in Table 1. The mean parameter values averaged across all specific binding regions were K_1=0.166 $\pm$ 0.026 mL/min/mL, k_3'=0.242 $\pm$ 0.086 min^{-1}, k_4=0.115 $\pm$ 0.022 min^{-1}, and V_b=0.04 $\pm$ 0.004 mL/mL. The average percent standard fitting errors were K_1 (5), k_3' (38), k_4 (42), BP_{CM} (5), and V_b (33). The estimated BP_{CM} values (Table 2) were largest in amygdala, thalamus, and basal ganglia, moderate in cingulate and peri-acqueductal gray matter, and lowest in cerebellum and cortical regions, which is consistent with the known distribution of μ-opioid receptors (Pfeiffer et al., 1982).

3.3. Estimation of binding potential

The regional binding potential estimates obtained with all methods (Table 2) showed excellent correlation (r >0.97) with each other. For BP_{CM} values less than 1.5, BP_{LR} and BP_{SRTM} were within 5% of $BP_{CM.}$ However, for large values ($BP_{CM} > 3$) both BP_{LR} and BP_{SRTM} underestimated BP_{CM} by more than 10%. Conversely, BP_{RATIO} overestimated BP_{CM} by over 30%, except for high binding regions (BP_{CM}>3) where the percent differences were

Table 2
Regional CFN binding potential (BP) estimates in control subjects (n=6) using six different methods as described in the text

Input Function	BP_{CM} Blood	BP_L Blood	BP_{SRTM} OCC	BP_{LR} OCC	BP_{RATIO} OCC	BP_{R2TM} OCC
Amygdala	3.91 (0.7)	3.64 (0.6)	3.16 (0.5)*	2.98 (0.4)*	3.80 (0.7)	3.78 (1.3)
Thalamus	3.89 (0.9)	3.82 (0.8)	3.52 (0.7)*	3.47 (0.6)*	4.61 (1.0)*	3.90 (1.0)
Caudate	3.84 (1.3)	3.76 (1.3)	3.35 (0.9)*	3.31 (0.9)*	4.32 (1.1)*	3.76 (1.0)
Putamen	2.53 (0.8)	2.54 (0.8)	2.38 (0.7)	2.41 (0.7)	3.15 (0.9)*	2.47 (0.7)
Cingulate	1.71 (0.6)	1.71 (0.6)	1.64 (0.4)	1.64 (0.5)	2.26 (0.8)*	1.71 (0.5)
Peri-acqueductal	1.70 (0.6)	1.69 (0.7)	1.55 (0.4)*	1.55 (0.5)*	2.25 (0.5)*	1.62 (0.5)
Cerebellum	1.33 (0.1)	1.38 (0.2)	1.33 (0.2)	1.35 (0.2)	1.78 (0.3)*	1.36 (0.2)
Temporal cortex	1.25 (0.4)	1.29 (0.4)	1.22 (0.3)	1.24 (0.4)	1.69 (0.6)*	1.26 (0.4)
Frontal cortex	1.25 (0.5)	1.27 (0.5)	1.21 (0.4)	1.23 (0.4)	1.66 (0.7)*	1.22 (0.5)
Parietal cortex	1.06 (0.3)	1.09 (0.3)	1.05 (0.2)	1.06 (0.2)	1.42 (0.5)*	1.05 (0.3)

There are two blood-based methods including compartmental modeling (BP_{CM}) and the graphical method of Logan (BP_L). Reference tissue methods include a simplified reference-tissue model (BP_{SRTM}), the Logan graphical method (BP_{LR}), a tissue ratio method (BP_{RATIO}), and a modification of the simplified reference-tissue model that uses two tissue compartments to represent the reference region (BP_{R2TM}). Standard deviations are shown in parentheses.

* Significantly different from BP_{CM} ($p<0.05$).

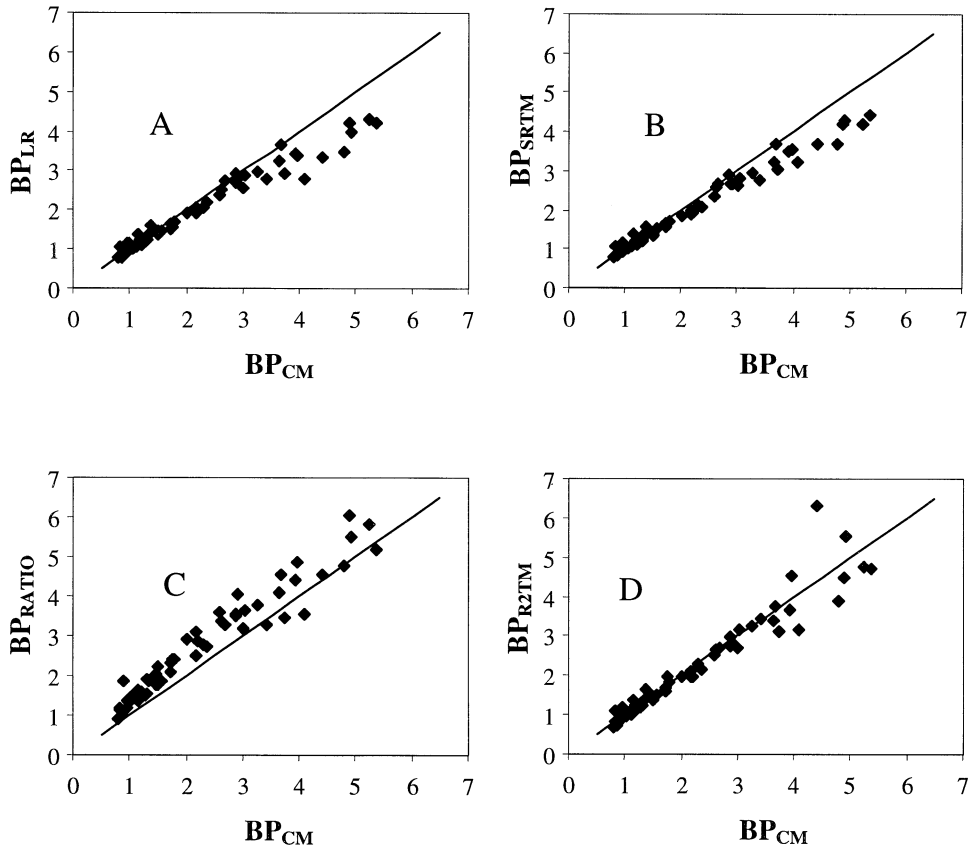

Fig. 5. Comparison of binding potential (BP) estimates obtained with reference-tissue methods versus those obtained using blood input compartmental modeling. Each plot shows the BP values measured in ten specific binding regions in six different subjects, giving a total of 60 measurements. The x-axis for each plot is BP_{CM}, the BP estimate obtained using blood input compartmental modeling. The y-axis shows the BP estimates obtained using A: Logan graphical analysis with occipital cortex (OCC) input (BP_{LR}), B: a simplified reference-tissue model (BP_{SRTM}), C: Tissue-ratio method (BP_{RATIO}), D: Modified version of the simplified reference-tissue model in which two-tissue compartments are used for the reference region (BP_{R2TM}).

smaller. BP_L showed excellent agreement with BP_{CM}, with BP estimates from the two methods having mean differences of less than 4% for all but one region. The values of BP_{LR} measured with $k_2' = 0$ were within 1% of those measured with $k_2' = 0.104$ min^{-1}, which was the mean value of k_2' obtained from compartmental modeling. Both graphical measures (BP_L and BP_{LR}) gave somewhat better agreement with BP_{CM} when the linear slope was measured from 30-90 min, instead of 10-90, or 20-90 min (not shown). BP_{R2TM} showed almost no bias, however, there is larger uncertainty for this method, especially at higher values (Figure 5).

3.4. Simulations

Parameter values used to generate simulated time-activity curves were V_e=1.59 mL/mL, k_3'=0.15, 0.25, 0.35 min^{-1}, k_4=0.115 min^{-1}, and V_b=0.04 mL/mL. To simulate different rates of blood flow, K_1 was varied from 0.05 ml/min/ml to 0.5 ml/min/ml, which encompassed the range of fitted K_1 values (0.101-0.266 ml/min/ml). Since V_e is held fixed, K_1 and k_2' were in effect varied simultaneously. For each simulated specific binding curve, a corresponding reference-tissue curve was simulated using a one-tissue model (Figure 1A), with $K_1^r = K_1$ and $k_2^r = k_2'$. Figure 6 shows the effect of blood flow on the BP estimates obtained from reference-tissue based analyses of simulated time-activity curves. Reference-tissue modeling was found to be relatively insensitive to flow. Reference-tissue graphical analysis is also fairly insensitive to flow, although there is a tendency for the graphical method to underestimate BP at low flow rates. The tissue-ratio method shows a comparatively larger dependence on blood flow, with an underestimation of BP at $K_1 = 0.05$ ml/min/ml, but substantial overestimation of BP for $K_1 > 0.15$ ml/min/ml.

3.5. Mouse studies

HPLC analysis of mouse plasma (n = 3) at 20 min following adminstration of CFN showed a similar metabolite profile to that seen in human plasma, including a lipophilic metabolite peak that elutes shortly after CFN. However, no trace of the lipophilic metabolite was found in the mouse brain extract, which contained only CFN (Figure 7).

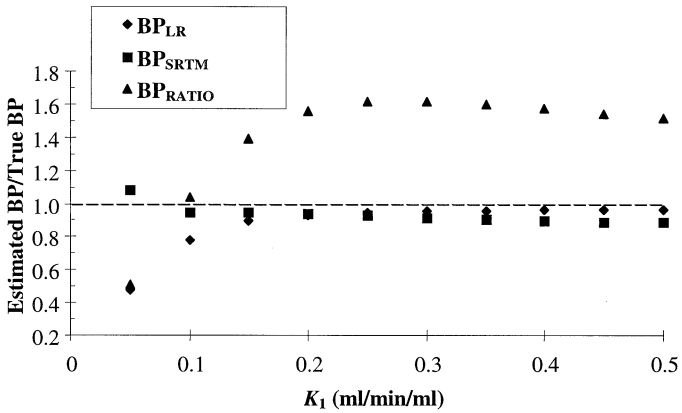

Fig. 6. Effects of blood flow on estimation of BP using reference-tissue methods. Curves were simulated with V_e=1.59 ml/mL, k_3'=0.25 min^{-1}, k_4=0.115 min^{-1}, and V_b=0.04 ml/mL. K_1 was varied from 0.05-0.5 ml/min/ml, which encompasses the range of fitted K_1 values (Table 1). For each K_1 value a reference curve was simulated with V_e=1.59 ml/mL, k_3'=0.0 min^{-1}, and V_b=0.04 ml/mL. A metabolite-corrected blood input function obtained from a PET study was used. To estimate binding potential, simulated curves were analyzed with the following reference-tissue methods: graphical analysis ◆, reference-tissue compartmental modeling ■, and the tissue-ratio method ▲. The results are displayed as the ratio of the estimated and true binding potential values. For comparison, the dashed line indicates the ideal ratio of 1. The tissue-ratio method shows a much greater bias in estimation of BP, and a larger sensitivity to blood flow than the other reference-tissue methods. These effects were also observed in simulations with k_3=0.15, and 0.35 min^{-1} (not shown).

4. Discussion

4.1. [^{11}C]carfentanil metabolites

Although the metabolism of several synthetic opioids has been well documented, the metabolites of carfentanil have not been identified. However, since this class of synthetic opioids bears strong structural similarities it is possible to infer the nature of CFN metabolites. The major metabolic path for this class is N-dealkylation, which removes the lipophilic phenylethyl group and yields the more polar species norfentanyl from fentanyl [14], and noralfentanil from alfentanil [13]. Thus the major CFN metabolite eluting at 1.6 min following column switch would be norcarfentanil, which still contains the [^{11}C]-methyl group. The appearance of the lipophilic CFN metabolite that eluted at 7.0 min may be construed to correspond to loss, again by N-dealkylation, of the more polar phenylpropionamide group, which occurs in alfentanil [13], but not in fentanyl, since fentanyl does not contain a substituent at C4 of the piperidine ring [14]. The loss of the polar group would yield a species slightly more lipophilic than carfentanil and still bearing the [^{11}C]-methyl group. Fortunately, the mice studies indicate that this metabolite does not enter the brain, thus will not confound the analysis of brain tissue curves.

4.2. Reference-tissue methods

Both reference-tissue modeling (BP_{SRTM}) and reference-tissue graphical analysis (BP_{LR}) gave BP estimates that are highly correlated with those obtained from compartmental modeling (BP_{CM}) and show little bias. However, there was a tendency for BP_{SRTM} and BP_{LR} to underestimate BP_{CM}, especially in high binding regions. The underestimation of BP_{CM} when using graphical analysis is consistent with a systematic underestimation by BP_L due to statistical noise that is most severe when BP is large [21]. The simulations showed that underestimation of BP by the graphical method (BP_{LR}) was most significant at low flow rates, which is consistent with a slower approach to linearity of the graphical plot. The greater bias found when measuring the graphical slope from 10-90 min, as opposed to 30-90 min, can also be attributed to a delayed approach to linearity [5]. The near equivalent BP_{LR} estimates obtained with $k_2' = 0$, and k_2' set to a mean measured value, indicates that the k_2' term need not be included when applying the graphical method to CFN. A modified reference-tissue method (BP_{R2TM}) gave unbiased estimates of BP_{CM}, however, the variability of the estimate appears too high to be of practical use (Figure 5). Compared to reference-tissue modeling and graphical analysis, the BP estimates obtained with the tissue-ratio method showed a much larger bias relative to BP_{CM}, as well as a greater sensitivity to blood flow. Therefore, of the reference-tissue methods that were examined, the tissue-ratio method is the least desirable for quantification of [^{11}C]carfentanil binding potential. In the original study that validated the tissue-ratio method against a more rigorous compartmental modeling technique, the primary basis for comparison was the strong correlation between the two measures ($r = 0.98$). A similarly high correlation between BP_{RATIO} and BP_{CM} was also found in the present study. However, since the analysis includes regions with a large range of receptor densities, a high correlation does not provide much more than a qualitative assessment that the methods will agree which regions have the lowest and highest binding levels. Furthermore, the correlation of BP_{CM} with all other measures was virtually the same ($0.97 < r < 0.99$), and thus the correlation coefficient is not useful for distinguishing the methods. In addition, all methods should be similarly affected by the presence of a small

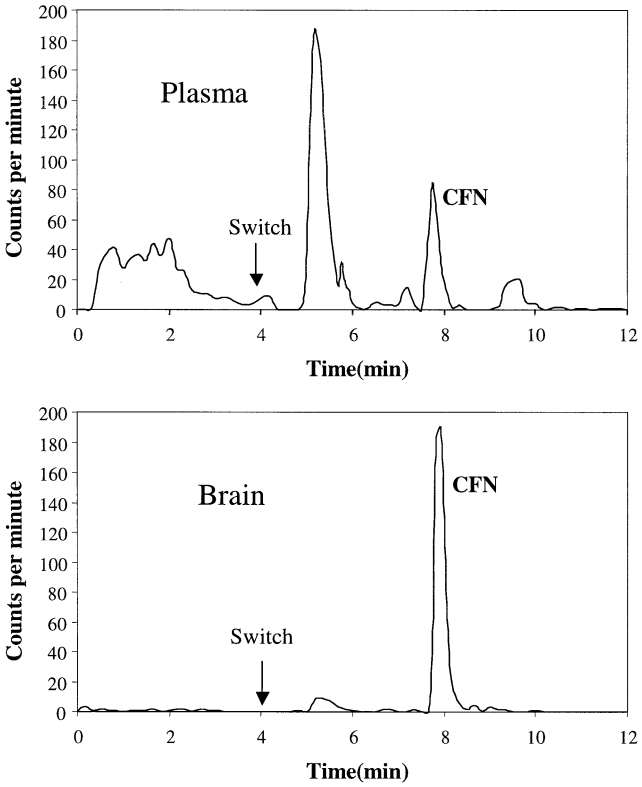

Fig. 7. HPLC chromatograms of mouse plasma (top) and brain (bottom) at 20 min following intraperitoneal injection of CFN. The radioactive metabolite profile observed in mouse plasma is similar to that seen in human plasma (Figure 2), which includes a large metabolite peak that elutes prior to CFN, and a lipophilic metabolite that elutes shortly after CFN. In mouse brain the lipophilic metabolite is absent, and nearly all radioactivity corresponds to the CFN peak.

specific binding component in the OCC reference region. In particular, specific binding in OCC would give an apparent increase in non-specific binding, which would reduce specific binding estimates. There are reportedly negligible μ-opioid receptors in OCC [9], however, even in that case it is possible for some specific binding to be artifactually introduced via partial volume effects. Since the apparent specific binding in OCC is expected to be small, any variability of this effect across studies should not significantly affect quantitative analyses.

4.3. Bias of tissue-ratio method

To better understand the overestimation of BP by the tissue-ratio method, we examined the accuracy of distribution volume estimates obtained from tissue-plasma ratios. As shown in Figure 8, the tissue-plasma ratio is not a very accurate measure of total distribution volume (V_T), and the accuracy is highly dependent on receptor density and blood flow. For a region with no specific binding the tissue-plasma ratio overestimates V_T at low flow rates, but gives a reasonable approximation of V_T at high flow rates. For regions with high specific binding the tissue-plasma ratio substantially overestimates V_T, except at very low flow rates. This systematic overestimation of V_T by the tissue-plasma ratio occurs when the slowest component of plasma clearance is comparable to or greater than the slowest tissue clearance rate [2]. Since high specific binding leads to slower tissue clearance, V_T is overestimated to a greater extent in high binding regions, which leads to greater overestimation of BP when using the tissue-ratio approach. Note that at very low flow rates the tissue-plasma ratio actually yields a smaller overestimation of V_T in a high binding region, as compared with a region with no specific binding (Figure 8). This effect occurs because a low flow rate leads to smaller tissue uptake, and less accumulation of tracer in the specific binding compartment, which limits the potential overestimation of V_T by the tissue-plasma ratio. The effects of tissue kinetics on estimating V_T with the tissue-ratio method can be virtually eliminated by using a continuous infusion paradigm for tracer delivery [2].

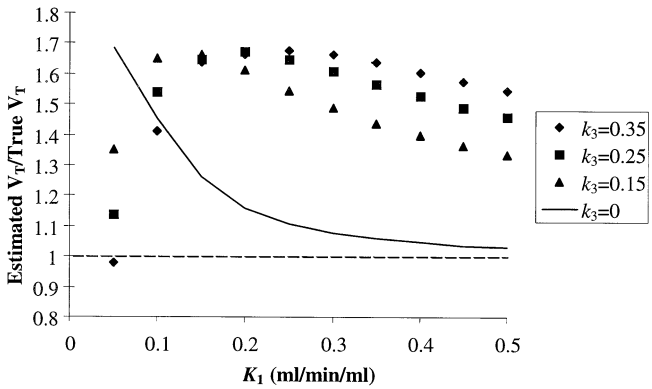

Fig. 8. The effects of blood flow on the estimation of [^{11}C]carfentanil distribution volume (V_T) using the tissue-plasma ratio. For this evaluation simulated tissue time-activity curves and plasma activity were averaged from 34-82 min. Parameter values for the simulated curves are given in Figure 6. Results are expressed as the tissue-plasma ratio divided by the true distribution volume. The dashed line indicates the ideal ratio of 1. The solid line corresponds to a tissue region with no specific binding ($k_3'=0$), for which he tissue-plasma ratio gave a better estimate of V_T as blood flow increased. In regions with specific binding ($k_3'=0.15$ (▲), 0.25 (■), 0.35 min^{-1} (◆) the tissue-plasma ratio substantially overestimates V_T for nearly all simulated curves.

4.4. Similarity between the graphical method and SRTM

The most suitable reference-tissue measures of CFN specific binding are BP_{SRTM} and BP_{LR}, because they both show low variability, with a limited bias (~10%) that is seen mainly in high binding regions. In fact the agreement between BP_{SRTM} and BP_{LR} is quite striking, as their mean regional values agree to two significant digits for all but one region (Table 2). This is not surprising as both the Logan graphical method and the SRTM equation are derived from the same underlying principles. In particular, both methods assume that the tracer rapidly equilibrates among tissue compartments, even in tissue regions with high specific binding. For SRTM this assumption requires that the free, non-specific, and specific binding compartments are kinetically indistinguishable and thus can be modeled explicitly as a single compartment. For graphical analysis the compartmental description of the tissue kinetics is not specified, but it is assumed that at some time $t>t^*$ equilibrium will be achieved among tissue compartments after which the total distribution volume can be measured. Thus graphical analysis, like SRTM, effectively assumes that the tissue uptake behaves kinetically as a single compartment. Multilinear equations have been derived from graphical analysis [11] and the SRTM equation [23] clearly showing that mathematically these methods are virtually identical when the assumption of rapid equilibrium among tissue compartments holds true.

For parametric imaging, Logan graphical analysis is a very suitable method as linear fitting is robust even given the high noise levels in voxel data. A drawback of the graphical method is choosing the start time (t*) to be used for linear fitting. In the present study it was found that a later value ($t^*=30$ min) gave less bias than an earlier value ($t^*=10$ min), however, setting t* to a later value also means that fewer data are being used for the fit. For the analysis of ROI data, which usually have low noise levels, it is often acceptable to use fewer data and reduce the bias. For parametric imaging, t* should be set to an earlier value to help reduce variability due to the higher noise levels. For the SRTM method all the data are used for the analysis, and an efficient parametric imaging technique using basis functions has been developed such that SRTM may be applied without the need for non-linear regression [8]. Recently, an alternative parametric technique has been described that is based on a multilinear solution of the SRTM equation [23].

5. Conclusions

Several methods for quantification of CFN specific binding have been evaluated. The results show that all methods yield estimates of specific binding that are highly correlated with BP estimates obtained from compartmental modeling with a blood input function. However, the tissue-ratio method gave a substantial overestimation of binding potential, especially at high BP values, and had a non-trivial dependence on blood flow. Reference-tissue modeling and reference-tissue graphical analysis were in much better agreement, with only a minor dependence on blood flow. Although there is a small tendency for reference-tissue modeling and graphical analysis to underestimate BP, especially for large BP values, either of these methods appear suitable for quantification of CFN binding.

Acknowledgments

The authors wish to thank Hayden Ravert, John Musachio, Bob Smoot, William Matthews, and Robert Dannals for radioisotope production and radiochemical synthesis, David Clough and Karen Edmonds for their assistance with the PET studies, and Alexis J. Simich for administrative support. This study was supported by NIH grants RO1 AA11855-01, and 1 RO1 AA11872-01A2.

References

[1] H. Akaike, An information criterion (AIC), Math Sci 14 (1976) 5–9.
[2] R.E. Carson, M.A. Channing, R.G. Blasberg, B.B. Dunn, R.M. Cohen, K.C. Rice, P. Herscovitch, Comparison of bolus and infusion methods for receptor quantitation: application to [^{18}F]cyclofoxy and positron emission tomography, J Cereb Blood Flow Metab 13 (1993) 24–42.
[3] R.F. Dannals, H.T. Ravert, J.J. Frost, A.A. Wilson, H.D. Burns, H.N. Wagner, Jr, Radiosynthesis of an opiate receptor binding radiotracer: [C11]Carfentanil, Int J Appl Radiat Isot 36 (1985) 303–306.
[4] T.R. Degrado, T.G. Turkington, J.J. Williams, C.W. Stearns, J.M. Hoffman, R.E. Coleman, Performance characteristics of a whole-body PET scanner, J Nucl Med 35 (1994) 1398–1406.
[5] C.J. Endres, R.E. Carson, Assessment of dynamic neurotransmitter changes with bolus or infusion delivery of neuroreceptor ligands, J Cereb Blood Flow Metab 18 (1998) 1196–1210.
[6] J.J. Frost, H.N. Wagner, Jr, R.F. Dannals, H.T. Ravert, J.M. Links, A.A. Wilson, H.D. Burns, D.F. Wong, R.W. McPherson, A.E. Rosenbaum, M.J. Kuhar, S.H. Snyder, Imaging opiate receptors in the human brain by positron tomography, J Comput Assist Tomogr 9 (1985) 231–236.
[7] J.J. Frost, K.H. Douglass, H.S. Mayberg, R.F. Dannals, J.M. Links, A.A. Wilson, H.T. Ravert, W.C. Crozier, H.N. Wagner, Jr, Multicompartmental analysis of [11C]-carfentanil binding to opiate receptors in humans measured by positron emission tomography, J Cereb Blood Flow Metab 9 (1989) 398–409.
[8] R.N. Gunn, A.A. Lammertsma, S.P. Hume, V.J. Cunningham, Parametric imaging of ligand-receptor binding in PET using a simplified reference region model, NeuroImage 6 (1997) 279–287.
[9] J.M. Hiller, L.Q. Fan, Laminar distribution of the multiple opioid receptors in the human cerebral cortex, Neurochem Res 21 (1996) 1333–45.
[10] J. Hilton, F. Yokoi, R.F. Dannals, H.T. Ravert, Z. Szabo, D.F. Wong, Column-switching HPLC for the analysis of plasma in PET imaging studies, Nucl Med Biol 27 (2000) 627–630.
[11] M. Ichise, J.R. Ballinger, H. Golan, D. Vines, A. Luong, S. Tsai, H.F. Kung, Noninvasive quantification of dopamine D2 receptors with Iodine-123-IBF SPECT, J Nucl Med 37 (1996) 513–520.
[12] R.A. Koeppe, V.A. Holthoff, K.A. Frey, M.R. Kilbourn, D.E. Kuhl, Compartmental analysis of [11C]flumazenil kinetics for the estimation of ligand transport rate and receptor distribution using positron emission tomography, J Cereb Blood Flow Metab 11 (1991) 735–44.

[13] R.B. Labroo, M.F. Paine, K.E. Thummel, E.D. Kharasch, Fentanyl metabolism by human hepatic intestinal cytochrome P450 3A4: implications for interindividual variability in disposition, efficacy, and drug interactions, Drug Metab Dispos 25 (1997) 1072–1080.

[14] R.B. Labroo, K.E. Thummel, K.L. Kunze, T. Podoll, W.F. Trager, E.D. Kharasch, Catalytic role of cytochrome P4503A4 in multiple pathways of alfentanil metabolism, Drug Metab Dispos 23 (1995) 490–496.

[15] A.A. Lammertsma, C.J. Bench, S.P. Hume, S. Osman, K. Gunn, D.J. Brooks, R.S. Frackowiak, Comparison of methods for analysis of clinical [11C]raclopride studies, J Cereb Blood Flow Metab 16 (1996) 42–52.

[16] A.A. Lammertsma, S.P. Hume, Simplified Reference Tissue Model for PET Receptor Studies, NeuroImage 4 (1996) 153–158.

[17] J. Logan, J.S. Fowler, N.D. Volkow, A.P. Wolf, S.L. Dewey, D.J. Schyler, R.R. MacGregor, R. Hitzemann, B. Bendriem, S.J. Gatley, D. Christman, Graphical analysis of reversible radioligand binding from time-activity measurements applied to [N-^{11}C-methyl]-(-)-Cocaine: PET studies in human subjects, J Cereb Blood Flow Metab 10 (1990) 740–747.

[18] J. Logan, J.S. Fowler, N.D. Volkow, G.J. Wang, Y.S. Ding, D.L. Alexoff, Distribution volume ratios without blood-sampling from graphical analysis of PET data, J Cereb Blood Flow Metab 16 (1996) 834–840.

[19] C.C. Meltzer, R.N. Bryan, H.H. Holcomb, A.W. Kimball, H.S. Mayberg, B. Sadzot, J.P. Leal, H.N. Wagner, Jr, J.J. Frost, Anatomical localization for PET using MR imaging, J Comput Assist Tomogr 14 (1990) 418–426.

[20] A. Pfeiffer, A. Pasi, P. Mehraein, A. Herz, Opiate receptor binding sites in human brain, Brain Res 248 (1982) 87–96.

[21] M. Slifstein, M. Laruelle, Effects of statistical noise on graphic analysis of PET neuroreceptor studies, J Nucl Med 41 (2000) 2083–2088.

[22] H. Watabe, R. Carson, H. Iida, The reference tissue model: Three compartments for the reference region, NeuroImage 11 (2000) S12.

[23] Y. Zhou, C.J. Endres, J.R. Brasic, S-C. Huang, D.F. Wong, Linear regression with spatial constraint to generate parametric images of ligand-receptor dynamic PET studies with a simplified reference tissue model, NeuroImage, in press.